JOURNAL OF COLLOID AND INTERFACE SCIENCE 155, 319–324 (1993)

Noninvasive Study of Gel Formation in Polymer-Stabilized Dense Colloids Using Multiply Scattered Light

P. D. KAPLAN[1] AND A. G. YODH

Physics Department, University of Pennsylvania, Philadelphia, Pennsylvania 19104

AND

D. F. TOWNSEND

Hercules Incorporated, Hercules Research Center, Wilmington, Delaware

Received June 8, 1992; accepted August 11, 1992

We use diffusing-wave spectroscopy to monitor the evolution of a colloidal gel. Changes in particle diffusion are resolved without perturbing the system and are used to distinguish between unstable and stable emulsions during the early stages of their development. Our observations suggest that multiple-scattering spectroscopies may be a valuable diagnostic of an industrially useful dispersion.

I. INTRODUCTION

Gel formation from colloidal suspensions is a well known but incompletely understood phenomenon. It can be useful, for example, in paints, where polymer gel networks create stable structures after being applied. On the other hand, gel formation can ruin emulsion products that must remain stable prior to use. The development of a gel from a colloid depends on many factors, including chemical kinetics and particle or polymer diffusion. Because of this complexity, it is important to develop *in situ* probes of evolving gels. Traditional rheologic techniques for studying these systems mechanically perturb them, altering the systems' evolution. Optical techniques have been largely limited to use in dilute systems as a result of interpretational difficulties associated with multiple scattering. The development of structure within alkyl ketene dimer (AKD) emulsions, which are used as paper size, becomes a concern to suppliers and customers alike if the systems become too thick to pump. Early recognition of gel formation can help ensure that there are no material losses at the paper mills.

In this work we use light *multiply scattered* from dense suspensions of AKD to study the gradual development of gel structure. Our measurements resolve average particle displacements in the sample. The data reveal qualitative changes in the nondiffusive motion of AKD particles. These changes arise because the growing gel network effectively traps the colloidal particles. Thus, measurements of particle diffusion provide insight into the process by which gels develop and offer a sensitive way to identify the degradation of a suspension.

Several traditional approaches to the study of dispersion stability are less appropriate for AKD. Standard measurements of bulk kinematic viscosity by rotational viscometers strongly perturb the system and are only useful for detecting gel structures in advanced stages. Dynamic rheology, such as the approach used by Tadros (1), works better at higher volume fractions or for more fully developed structures. Quasi-elastic light scattering, laser diffraction, and optical microscopy require dilution, altering the system's adsorption equilibrium. The small difference in density between the particles and the continuous phase eliminates acoustic methods and creaming/settling techniques. On the other hand, we shall demonstrate that multiple light scattering (2) works without dilution, does not perturb the sample, and provides quantitative information about particle motion even at early stages of the thickening process.

Ketene dimer emulsions have several characteristics making them ideal for this study. The AKD system is a homogenized distribution of particles whose average diameter is $\approx 0.4\ \mu m$. The particles have almost the same density as water and do not sediment or cream (3). The dispersion exhibits strong multiple scattering and can form a gel at surprisingly low particle concentrations (4). Because the unstable suspensions thicken more slowly at room temperature and more rapidly when kept warm (4), we have been able to control this system so that the gel evolves gradually over a period of several days. This controlled rate of evolution has allowed us to see stages of the gel's evolution.

Alkyl ketene dimers are used in the manufacture of paper to control the penetration of the water into the sheet. These

[1] To whom correspondence should be addressed.

0021-9797/93 $5.00

materials are not soluble in water and must be dispersed to be compatible with the aqueous environment of the pulp slurry. To be useful, the suspensions must be stabilized against aggregation so that they are pumpable, dilutable, and free of large clumps. As a result, the stability of AKD is industrially significant, and the applicability of multiple-scattering spectroscopies to this system demonstrates a practical use of this new method.

II. DIFFUSING-WAVE SPECTROSCOPY

Diffusing-wave spectroscopy (DWS) is an optical, multiple-scattering technique with tremendous promise for colloidal science (2). The technique has been used successfully to observe concentration dependent particle diffusion in monodisperse colloids (5), diffusion and structure in binary colloids (6), very early time Brownian dynamics of single particles (8), gelation of cottage cheese (9), and glass transitions in charged dispersions (10). The data derived from DWS, like the data from traditional light scattering, reveal the time evolution of the average particle displacement. We will briefly review the fundamental results of DWS with the assumption that the reader is familiar with traditional quasi-elastic light-scattering techniques (11). Although the discussion that follows applies to monodisperse suspensions, the results can be generalized to polydisperse suspensions by using an average diffusion coefficient. More complete explanations of DWS are found in Refs. (12) and (13).

The apparatus required for DWS studies is essentially the same as for quasi-elastic light scattering, although the optics are simpler. The optical setup for DWS is shown in Fig. 1. A colloidal dispersion, as opaque as milk or white paint, is placed in a cuvette which is illuminated by a continuous wave laser. Light diffuses through the sample, and a diffraction-limited output speckle is imaged onto a photomultiplier tube. The measured speckle intensity $I(t)$ is fed to an electronic correlator which calculates the temporal intensity autocorrelation function: $g_2(\tau) = \langle I(\tau)I(0)\rangle/\langle I(0)\rangle^2 - 1$. Here the $\langle\ \rangle$ brackets denote time averages. This function

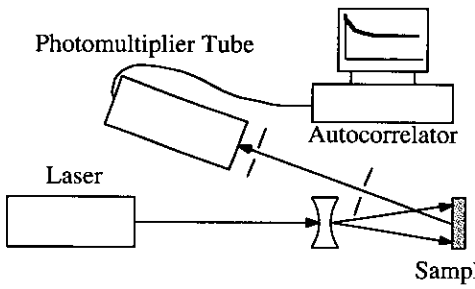

FIG. 1. Diffusing-wave spectroscopy apparatus. A wide beam of uniform intensity illuminates a slab of optically dense sample. A speckle of backscattered light is imaged onto a fiber which transmits to a photomultiplier tube. The temporal intensity autocorrelation is then computed by the correlator.

is simply related to the electric field autocorrelation function $g_1(\tau) = \langle E^*(0)E(\tau)\rangle/\langle |E(0)|^2\rangle$ by the Siegert relation (12) (i.e., $g_2(\tau) = |g_1(\tau)|^2$). We deduce information about sample particle dynamics from the shape of $g_2(\tau)$.

Recall the form of $g_1(\tau)$ in a single-scattering experiment (14):

$$g_1^{ss}(\tau) = \exp(-\frac{1}{6}q^2\langle\Delta r^2(\tau)\rangle) = \exp(-q^2D\tau), \quad [1]$$

where the scattering wavevector q is $2k_0\sin(\theta/2)$, θ is the scattering angle, k_0 is the wavevector of the incident light field in the solvent, $\langle\Delta r^2(\tau)\rangle$ is the mean square particle displacement in a time interval τ, and D is the particle diffusion coefficient. In multiple-scattering experiments, $g_1(\tau)$ is related to Eq. [1] in a relatively straightforward way. A typical photon undergoes a sequence of n scattering events before emerging from the sample. The trajectory of the photon is characterized by its total length s and the typical distance between scattering events l. Thus, $n = s/l$. If these scattering events are uncorrelated, then the phase shift (in time τ) of the output field can be derived from the phase shift due to a "typical" single-scattering event, raised to the nth power. The "typical" phase shift is calculated by averaging over all allowed momentum transfers q and over all particle displacements associated with the single-scattering event. The effects of different pathlengths (i.e., different n) must then be averaged together. Within these approximations, the expression for $g_1(\tau)$ is

$$g_1(\tau) = \int_0^\infty P(s)\exp(-\frac{1}{6}\langle\Delta r^2(\tau)\rangle\langle q^2\rangle_\Omega(s/l))ds$$
$$= \int_0^\infty P(s)\exp(-D\tau\langle q^2\rangle_\Omega(s/l))ds, \quad [2]$$

where $\langle q^2\rangle_\Omega$ is the angle-averaged, mean-square scattering vector for a typical scattering event in the scattering sequence, and $P(s)$ represents the probability that a photon will travel a distance s through the media before emerging. The interpretation of Eq. [2] is the key to DWS. By using an experimental geometry for which [2] has been analytically evaluated (12, 13), we can determine the short-time particle-diffusion coefficient from the correlation function. Equation [2] is strictly valid only for systems of independent particles with no photon absorption. We can generalize the result to include the effects of weak particle interactions and photon absorption, but we will not use those results here, except to note that backscattering experiments are significantly less sensitive to photon absorption than transmission experiments. To understand this difference in sensitivity, recall that backscattered photons travel much shorter distances inside the sample than transmitted photons and are thus less likely to be absorbed.

In this study, we use a plane-wave-input, point-output scattering geometry (see Fig. 1). Light is collected from a single speckle backscattered from a point near the center of a large input spot. In this case the expression for g_2 is

$$g_1^{\text{back}}(\tau) = \frac{\sinh[(L/l^* - z_0/l^*)\sqrt{6D\tau k_0^2}] + (2/3)\sqrt{6D\tau k_0^2}\cosh[(L/l^* - z_0/l^*)\sqrt{6D\tau k_0^2}]}{(4/3)\sqrt{6D\tau k_0^2}\cosh[(L/l^*)\sqrt{6D\tau k_0^2}] + (1 + (8/3)D\tau k_0^2)\sinh[(L/l^*)\sqrt{6D\tau k_0^2}]}, \quad [3]$$

so that for τ much less than $(6Dk_0^2)^{-1}(l^*/L)^2$,

$$\ln(g_1^{\text{back}}(\tau)) \approx 1 - A\sqrt{\tau} + B\tau + \mathcal{O}(\tau^{3/2}), \quad [4]$$

where the photon random walk step length is $l^* = 2lk_0^2/\langle q^2\rangle_\Omega$, D is the particle diffusion coefficient, z_0 is a parameter of the theory typically set to $4l^*/3$, and $A = \gamma\sqrt{6Dk_0^2}$ for unconstrained Brownian motion in the absence of photon absorption (15).

In contrast to quasi-elastic light scattering, the form of the data in DWS is the same for monodisperse and polydisperse samples (12). That is, the shapes of the decay curves are the same for all diffusive systems, and the measured diffusion coefficient in the polydisperse systems is an average over the coefficients from each particle species (6, 7). This makes the observation of gel formation or other phase changes signified by nondiffusive motion less ambiguous for DWS than quasi-elastic light scattering, even in complex, ill-defined systems.

III. MATERIALS AND METHODS

The primary goal of this experiment was to demonstrate that diffusing-wave spectroscopy can identify gel-forming suspensions. Accordingly, three samples of AKD emulsion were prepared, kept at 32°C, and monitored daily by DWS. Brookfield viscosity measurements were also performed to provide an independent rheological test of the colloidal stability of the samples at the experimental endpoints. The details of sample preparation, the diffusing-wave measurements, and the viscosity measurements are discussed below.

The DWS apparatus (see Fig. 1) operated in the backscattering mode. Samples in 2-mm-thick cuvettes were illuminated by the 514.5 nm line of an Ar-ion laser. A uniform input intensity profile was obtained by spatially filtering and expanding the laser beam, then allowing only the central third of the beam to strike the sample. A single speckle of output light was then collected from the center of the input spot. This speckle was imaged onto an optical fiber with a 50-μm core, which acts as a pinhole, and directed onto a photon-counting photomultiplier tube. The correlation function's temporal decay depends on only the experimental geometry and particle diffusion. A value of A was determined from each DWS decay curve by fitting the decay curve to Eq. [4] (16). Most of the discussion will center on the best-fit value of A, which reflects the average particle diffusion coefficient.

The emulsions of AKD were prepared using techniques outlined in the patent by Edwards and Townsend (4). Alkyl ketene dimer was blended with a starch and sodium lignin sulfonate mixture and homogenized at 65°C. Three samples were made at about 13% total solids. The resulting emulsion consists of a distribution of particles with an average diameter of $\approx$0.4 μm, but a range of diameters from roughly 0.1 to about 1.0 μm. The sulfonated lignin goes into solution with the starch, and together they stabilize the dispersion. It is not known whether stabilization is a result of steric hindrance or depletion. If the dispersion is made improperly, the sample viscosity is observed to increase in time, and the dispersion develops properties of a gel. Again, the mechanism for this phenomenon is not well understood, although it is believed to be brought about by polymer association. Examples of conditions that can make the AKD emulsions unstable are high levels of electrolyte, poorly cooked starch, and under or over homogenization. The conditions these suspensions

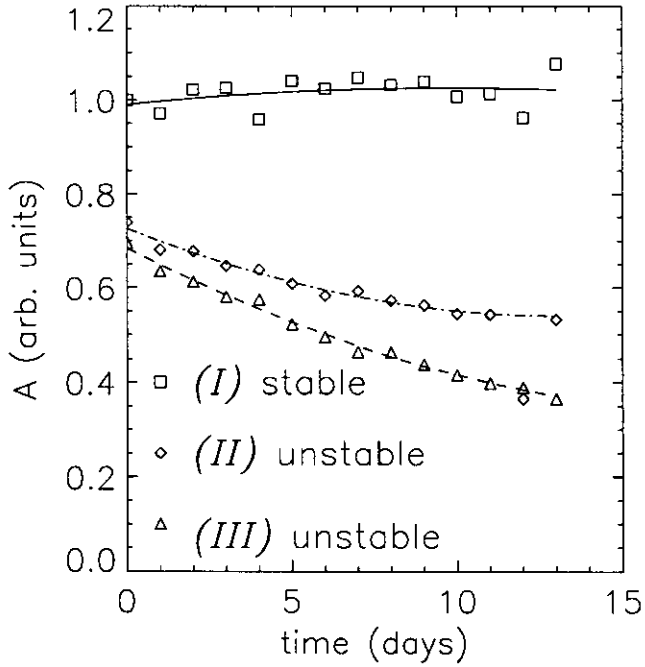

FIG. 2. Daily results of DWS measurements. Plotted is the value of the coefficient A from Eq. [4] measured on each day. The samples appear different on the first day, probably due to a difference in average particle size. The samples also clearly evolve differently. Lines are drawn to guide the eye. Squares, sample I. Diamonds, sample II. Triangles, sample III.

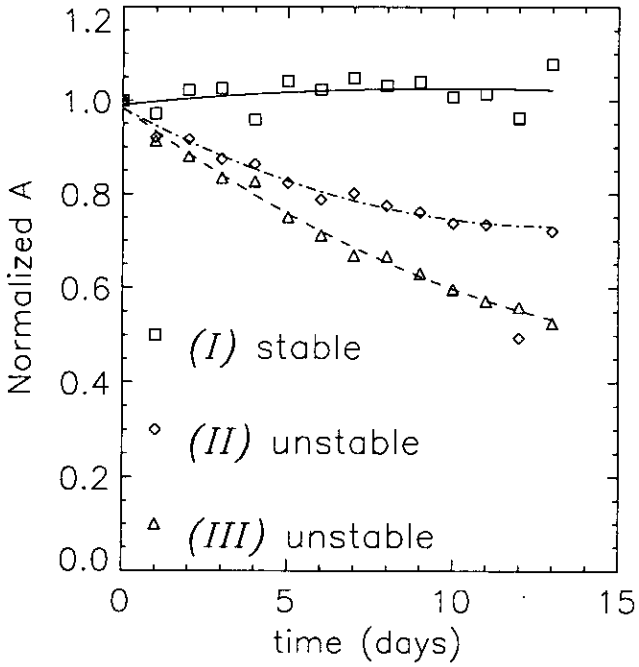

FIG. 3. Daily results of DWS measurements normalized to their value on the first day. This figure emphasizes the evolution of the unstable samples. Lines are drawn to guide the eye. Squares, sample I. Diamonds, sample II. Triangles, sample III.

were made under were intentionally varied to try to induce at least one of the suspensions to gel (4).

A Brookfield viscometer was used to measure relative sample stability initially and then after four weeks of aging at 32°C. During this time, a small quantity of each sample was tested daily using DWS.

IV. RESULTS AND DISCUSSION

The results were analyzed on two time scales. First, the *daily* changes in the fitting parameters were determined and used to answer questions of relative stability. Second, the *shape* of the backscattering decay curve on any given day was used to provide information about the dynamics of suspended particles on *microsecond* time scales. We will see that the particle diffusion rates in the unstable samples drop steadily over a two-week period, while the stable samples exhibit minimal changes. In addition, we find from the shape of $g_2(\tau)$ that the particle motion in all systems is nondiffusive on some time scale and that the nature of this nondiffusive motion changed significantly in the unstable samples during a two-week period.

The daily changes are shown in Fig. 2. The parameter A, derived from the decay curves, reflects changes in the average particle diffusion coefficient. It is quite apparent that sample particle diffusion in I, which was made to be "stable," changed very little over a two-week period, while diffusion in samples II and III, which were made to be "unstable," slowed down dramatically. Further, we can see that the decay rates on the first day differed by about 50%. This graph demonstrates that DWS can be used to distinguish between samples with the same Brookfield viscosity and total solids. In Fig. 3, we see the parameter A normalized to its value on

TABLE 1
Brookfield Viscosity Data Indicate the End-State of Our Three Samples

	Day 1		Day 7		Day 28	
	η (cp)	$\dot{\gamma}$ (s^{-1})	η (cp)	$\dot{\gamma}$ (s^{-1})	η (cp)	$\dot{\gamma}$ (s^{-1})
Sample I	13.0 ± 1	15.1			9.0 ± 1	15.1
Sample II	18.5 ± 1	15.1			135.0 ± 5	13.2
Sample III	15.0 ± 1	15.1	>500.0	13.2		

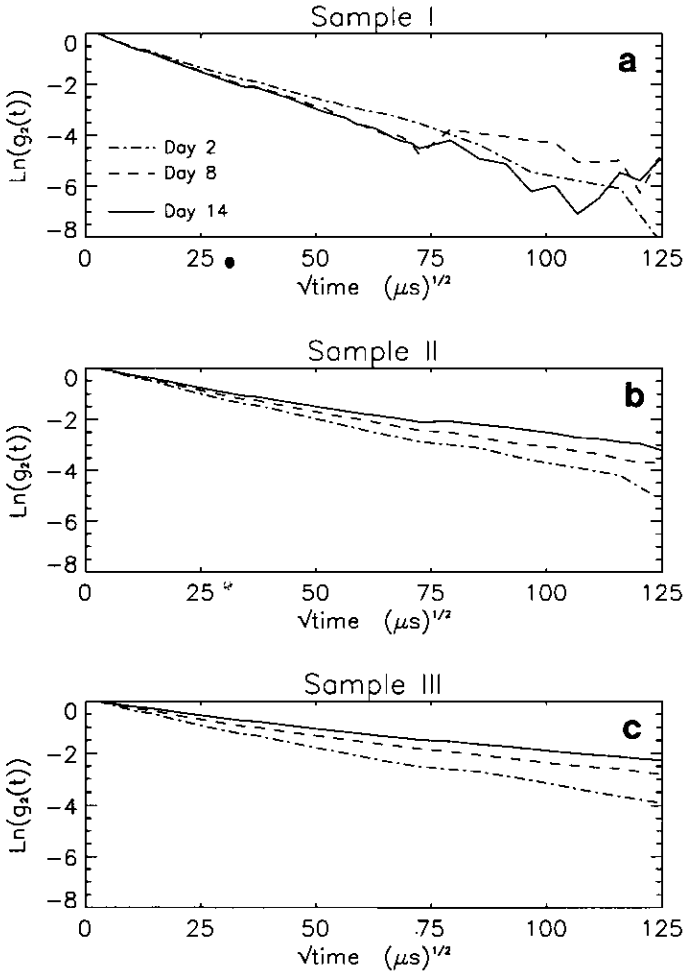

FIG. 4. Actual $g_2(\tau)$ curves. Each plot displays an early, intermediate, and late data set from one sample. (a) The long-term stability of sample I is indicated by the reproducibility of $g_2(\tau)$. (b, c) Samples II and III show changes in $g_2(\tau)$ over the course of several days. The dot–dashed line is from Day 2, while the dashed and solid lines are from Days 8 and 14, respectively.

the first day. This graph demonstrates that the *fractional change* in the unstable samples is substantially different from the stable one.

The Brookfield viscosity of these samples was measured at the experimental endpoints in order to demonstrate the dramatically different final states of these samples. The viscometer results for the three samples studied are shown in Table 1. Initially all of the samples exhibited a low viscosity, indicating a liquid state. After four weeks, sample I had not changed substantially, while samples II and III exhibited a large increase in viscosity. Sample III was clearly the least stable of the group, although sample II was also unstable. It should be noted that Brookfield viscosity is a bulk measurement unlike DWS, which reveals information about the *microscopic* dynamics of the sample. At the microscopic level, particles undergo Brownian motion even in a fully developed gel, but the dynamics in a gel are constrained by the gel's structure.

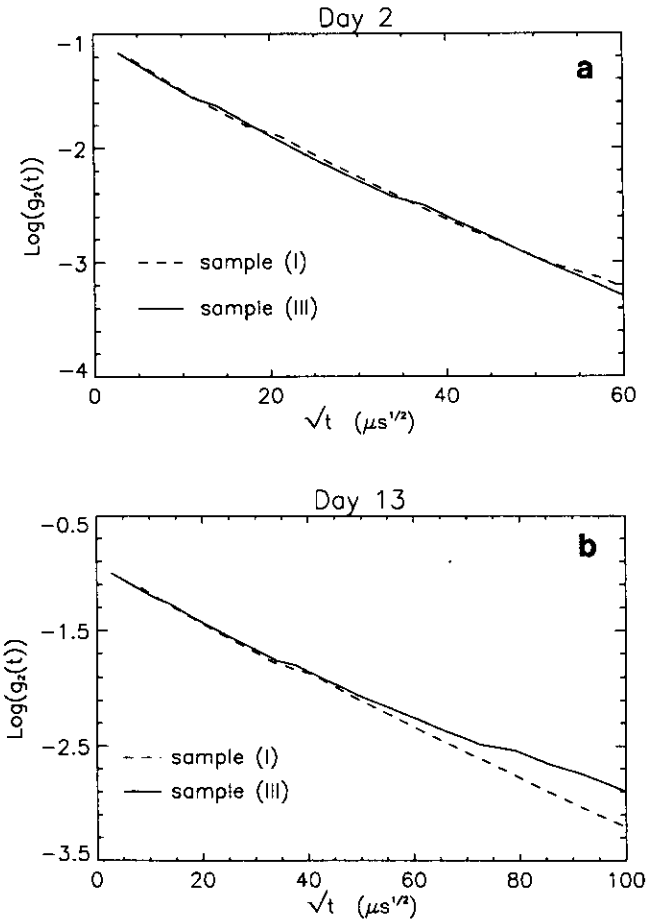

FIG. 5. Attempts to verify the form of $g_2(\tau)$ for different samples. The dashed line (from sample 1) is not plotted vs $\sqrt{\tau}$, but vs $\sqrt{\tau D_{III}/D_I}$. In (a) we see that, on the first few days of the experiment, the decay curves were related by a simple scaling argument, Eq. [5], while in (b) we see that by the end of the experiment this scaling argument failed. This failure is a quantitative measure of changes in the nondiffusive motion of the particles during gel formation.

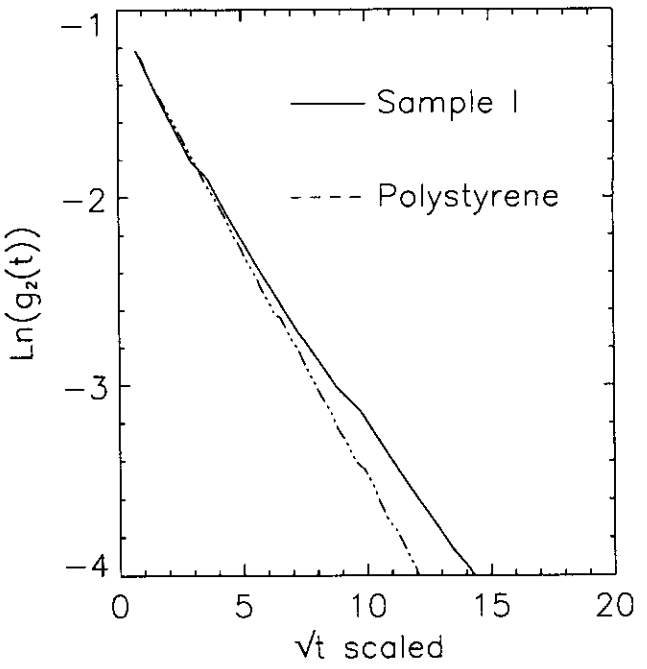

FIG. 6. Demonstration of constrained motion. Early data from sample I is shown along with an appropriately scaled (Eq. [5]) decay curve from a freely diffusing sample of polystyrene spheres in water. The upward curvature, observable in all backscattering data taken from the AKD suspensions, indicates that the particles were undergoing constrained Brownian motion.

In Fig. 4, the intensity autocorrelation function $g_2(\tau)$ is plotted for all three samples on different days. Changes in relative stability are indicated by growth in the distance between curves over the course of the experiment. This means that the particles in samples II and III were, on average, moving more slowly on the last day than on the first. We believe that this slowing is a signature of gel development. Our technique reveals that development over the course of several days.

We now examine the shape of the measured $g_2(\tau)$ curves to determine whether the particles in the sample were moving diffusively. The function $g_2(\tau)$ depends on the particle displacement $\langle \Delta r^2(\tau) \rangle$ (i.e., $g_2(\tau) = g_2(\langle \Delta r^2(\tau) \rangle)$). For diffusive motion $\langle \Delta r^2(\tau) \rangle = 6D\tau$. Thus, data taken from two samples (α and β) with different diffusion coefficients (D_α and D_β) are related to each other by

$$g_2^\alpha(\tau) = g_2^\beta\left(\frac{D_\alpha}{D_\beta}\tau\right). \qquad [5]$$

This is demonstrated by the overlap in the two lines in Fig. 5a, where $g_2(\tau)$ from sample I is plotted along with $g_2(D_I\tau/D_{III})$ from sample III (this data is from the second day of the experiment). *This scaling argument will fail, if the particle motion is of a qualitatively different form.* In Fig. 5b, we see a similar plot of data from Day 12, by which time the gel has had a strong effect on our DWS data. In this

figure, the scaling argument clearly fails. The separation between the two lines is a measure of the departure from diffusive motion.

It should be noted that *none* of these samples is ever freely diffusing. This can be seen in Fig. 6, where the scaling arguments of Eq. [5] are used to compare the AKD emulsions to data taken from freely diffusing 460-nm-diameter polystyrene spheres in water. Significant upward curvature of $g_2(\tau)$ from the AKD suspension indicates that the particles in samples I, II, and III were all undergoing constrained Brownian motion even on the first day of measurements. The fact that the three samples scale with each other indicates that, initially, the suspensions had similar microscopic dynamics, despite the fact that their average diffusion coefficients are different. The failure of scaling between samples I and III after several days is an indication of microscopic change in sample III. This change appears to be a precursor to the formation of a bulk gel.

V. SUMMARY

We have demonstrated the utility of DWS as a tool for diagnosing the stability of AKD emulsions. By examining the form of the DWS backscattering decay curve we have seen that in the unstable sample there is not just particle aggregation, but there are also qualitative changes in microscopic particle dynamics. In the future, it may be possible to compare the form of this data with results from dilute model gel systems that have been observed by single-scattering techniques (17). It is clearly desirable to directly compare rheological and DWS measurements on a daily basis. This comparison will provide detailed information about the processes by which these suspensions become unstable. Diffusing-wave spectroscopy is not simply a noninvasive probe, it is a sensitive and robust probe of microscopic motion in dense suspensions.

ACKNOWLEDGMENTS

We gratefully acknowledge discussions with D. J. Pine and H. N. Cheng. We thank M. H. Kao and R. Jones for their assistance in obtaining data and Derek Edwards for assistance in preparing the emulsions. This work was partially supported by the National Science Foundation through Grant DMR-9003687. AGY acknowledges partial support from the NSF through the PYI program and from the Alfred P. Sloan Foundation.

REFERENCES

1. Tadros, F. Th., *Langmuir* **6,** 28 (1990).
2. Stephen, M. J., *Phys. Rev. B* **37,** 1 (1988); Maret, G., and Wolf, P. E., *Z. Phys. B* **65,** 409 (1987); Pine, D. J., Weitz, D. A., Chaikin, P. M., and Herbolzheimer, E., *Phys. Rev. Lett.* **60,** 1134 (1988).
3. Caldwell, K. D., and Li, J., *J. Colloid Interface Sci.* **132,** 256 (1981).
4. Edwards, D. W., and Townsend, D. F., "High-Solids Alkyl Ketene Dimer Dispersion," US Patent 4861376, August 29, 1989.
5. Fraden, S., and Maret, G., *Phys. Rev. Lett.* **65,** 512 (1990); Qiu, X., Wu, X. L., Xue, J. Z., Pine, D. J., Weitz, D. A., and Chaikin, P. M., *Phys. Rev. Lett.* **65,** 516 (1990); Yodh, A. G., Kaplan, P. D., and Pine, D. J., *Phys. Rev. B* **42,** 4744 (1990).
6. Kaplan, P. D., Yodh, A. G., and Pine, D. J., *Phys. Rev. Lett.* **68,** 393 (1992).
7. The assumption of diffusive motion has been shown to work well in dense, monodisperse, hard-sphere systems as well; see for example the papers in Ref. (5), in which D depends on ϕ but the form of $g_2(\tau)$ does not depend on ϕ.
8. Weitz, D. A., Pine, D. J., Pusey, P. N., and Tough, R. J. A., *Phys. Rev. Lett.* **63,** 1747 (1989); Kao, M. H., Yodh, A. G., and Pine, D. J., *in* "Proc. Conference on Quantum Electronics and Laser Science (QELS '92), Anaheim, CA, May 10–15, 1992."
9. Dalgleish, D. G., and Horne, D. S., *Milchwissenschaft* **46,** 417 (1991).
10. Meller, A., and Stavans, J., *Phys. Rev. Lett.* **68,** 3646 (1992).
11. Pecora, R., "Dynamic Light Scattering." Plenum, New York, 1985.
12. Pine, D. J., Weitz, D. A., Zhu, J. X., and Herbolzheimer, E., *J. Phys. (France)* **51,** 2101 (1990).
13. MacKintosh, F. C., and John, S., *Phys. Rev. B* **40,** 2283 (1989).
14. Clark, N. A., Lunacek, J. H., and Benedek, G. B., *Am. J. Phys.* **38,** 575 (1970).
15. This coefficient depends on the value of z_0, taken here to be $4l^*/3$. The additional parameter γ was determined to be roughly 1.6 in the first article in Ref. (5).
16. It is necessary to fit to both A and B in Eq. [4]; the B term includes the curvature seen in Figs. 4–6. As displayed in Fig. 6, B is always larger for AKD samples than for freely diffusing spheres.
17. van Megen, W., Underwood, S. M., and Pusey, P. N., *Phys. Rev. Lett.* **67,** 1586 (1991); Xue, J. Z., Chaikin, P. M., and Pine, D. J., preprint. These authors use single-scattering QELS data from many small volumes of the sample in order to overcome ergodicity problems associated with a gel.